1-1-2000

The Optical Afterglow Light Curve of GRB 980519

Dieter H. Hartmann
Department of Physics and Astronomy, Clemson University, hdieter@clemson.edu

F. J. Vrba
US Naval Observatory, Flagstaff Station

A. A. Henden
US Naval Observatory, Flagstaff Station

B. Canzian
US Naval Observatory, Flagstaff Station

S. E. Levine
US Naval Observatory, Flagstaff Station

See next page for additional authors

THE ASTROPHYSICAL JOURNAL, 528:254–259, 2000 January 1

THE OPTICAL AFTERGLOW LIGHT CURVE OF GRB 980519

F. J. VRBA, A. A. HENDEN,[1] B. CANZIAN, S. E. LEVINE, C. B. LUGINBUHL, H. H. GUETTER, AND J. A. MUNN
US Naval Observatory, Flagstaff Station, P.O. Box 1149, Flagstaff, AZ 86002-1149

D. H. HARTMANN
Department of Physics and Astronomy, Clemson University, Clemson, SC 29634-1911

AND

M. C. JENNINGS[2]
P.O. Box 66, Corona del Mar, CA 92625

Received 1999 April 5; accepted 1999 August 10

ABSTRACT

We present *V*-, *R*-, and *I*-band observations made at the US Naval Observatory, Flagstaff Station, of the afterglow of GRB 980519 on UT 1998 May 20 and 22. These observations are combined with extensive data from the literature, and all are placed on a uniform magnitude system. The resultant *R*- and *I*-band light curves are fit by simple power laws with no breaks and indices of $\alpha_R = 2.30 \pm 0.12$ and $\alpha_I = 2.05 \pm 0.07$. This makes the afterglow of GRB 980519 one of the two steepest afterglows yet observed. The combined *B*-, *V*-, *R*-, and *I*-band observations are used to estimate the spectral power-law index, $\beta = 1.4 \pm 0.3$, after correction for reddening. Unfortunately, GRB 980519 occurred at a relatively low Galactic latitude ($b \approx +15$) where the Galactic reddening is poorly known and, hence, the actual value of β is poorly constrained. The observed α and range of likely β-values are, however, found to be consistent with simple relativistic blast-wave models. This afterglow and that of GRB 980326 displayed much steeper declines than the other seven well-observed afterglows, which cluster near $\alpha \approx 1.2$. GRB 980519 and GRB 980326 did not display burst characteristics in common that might distinguish them from the gamma-ray bursts with more typical light curves.

Subject headings: gamma rays: bursts — gamma rays: observations

1. INTRODUCTION

BeppoSAX (Boella et al. 1997) X-ray localizations of classical gamma-ray bursts (GRBs) to accuracies of a few arcminutes have produced an enormous breakthrough in our understanding of the nature of GRBs, allowing the afterglows of several GRBs to be detected and monitored at optical, infrared, and radio wavelengths. These latter observations have in turn produced localizations to better than an arcsecond and have led to the detection of faint blue galaxies at or very near the afterglow positions that may be the hosts of the GRB events. This linkage, along with direct redshift measurements of some of the optical afterglows, has established that at least most GRBs are of extragalactic origin. However, many outstanding problems remain regarding the nature of GRBs. The GRB fluences and large range in distances so far observed, from $z = 3.42$ for the putative host galaxy of GRB 971214 (Kulkarni et al. 1998) to $z = 0.0085$ for GRB 980425 (Lidman et al. 1998; Tinney, Stathakis, & Cannon 1998), imply a range in energy of more than 5 orders of magnitude. GRBs are energetically diverse, and/or relativistic beaming must be invoked to explain this apparently large range in energy. In addition to the neutron star merger model for GRBs (Paczynski 1991), the fact that GRB 980425 may have been associated with SN 1998bw (Galama et al. 1998a) adds the possibility that hypernovae may be responsible for at least some GRBs (Paczynski 1998).

Whatever the ultimate nature of GRBs, the afterglows thus far observed appear to be generally well understood in the context of relativistic blast-wave or fireball models (Mészáros & Rees 1997; Wijers, Rees, & Mészáros 1997; Sari, Piran, & Narayan 1998). In these models the afterglow radiation is due to synchrotron emission from electrons accelerated as the relativistic shock is slowed by its encounter with the circumburster medium. The simplest forms of these models (a spherical blast into a homogeneous medium) predict that, between the times when the synchrotron break frequency passes through the observing band and when the shock becomes nonrelativistic, the observed flux should drop as a simple power law of the form

$$F(t) = F_0 t^{-\alpha} . \qquad (1)$$

To date, sufficient optical data have been obtained for eight GRB afterglows other than GRB 980519 to allow reasonably well-sampled optical light curves to be constructed. The afterglow light curves of all of these GRBs are all well fit by power laws without breaks, as predicted by the above models. However, two of the GRBs show the diversity of the light curves soon after the GRB time. GRB 990123 was observed simultaneously in the optical (Akerlof & McKay 1999), reached peak brightness approximately 30 s after the burst, and continued a smooth power-law decline thereafter (Masetti et al. 1999). GRB 970508 was not observed simultaneously, so nothing is known of its prompt optical radiation, but reached an afterglow peak brightness between 1.1 and 1.8 days after the GRB and then continued along a smooth power-law decline (Sokolov et al. 1998). This demonstrates that little is yet known about the connection between prompt and afterglow radiation.

In this paper we present optical photometry for the afterglow of GRB 980519, obtained at the US Naval Observatory (USNO), Flagstaff Station. Combining our data with those published by others, we present well-sampled *R*- and

[1] Universities Space Research Association.
[2] Visiting Scholar, Institute of Geophysics and Planetary Physics, University of California, Riverside, Riverside, CA 92521.

TABLE 1
JOURNAL OF USNO OBSERVATIONS

UT Date (1998)	Filter	Start Time (UT)	Stop Time (UT)	Number of Exposures (10 minutes each)	Midpoint (UT 1998 May)
May 20......	*R*	03:35:39	04:11:20	3	20.1625
	R	04:59:31	05:52:54	3	20.2289
	V	05:56:21	06:31:05	3	20.2572
	R	06:33:20	07:18:25	3	20.2872
	R	10:13:51	11:07:55	5	20.4451
	I	04:15:09	07:52:39	6	20.2534
May 22......	*R*	03:39:21	07:57:44	23	22.2433

I-band light curves. The data show that GRB 980519 exhibited an afterglow which is well fit by a power law without breaks and which had one of the two steepest declines observed thus far.[3]

2. OBSERVATIONS

GRB 980519 (BATSE Trigger 6764) was detected by the *BeppoSAX* WFC (Piro 1998a), which provided a localization with an error radius of 3′ (Piro 1998b). An optical transient, discovered within the localization by Jaunsen et al. (1998), was found to fade rapidly in subsequent observations and was thus identified as the GRB afterglow. The afterglow position was coincident with a faint galaxy (Sokolov et al. 1998; Bloom et al. 1998b) presumed to be the host of the GRB event. We detected the afterglow, using the Flagstaff Station's 1 m telescope and a Tektronix 1024 × 1024 CCD Camera, on UT 1998 May 20 in single measurements in the Johnson *V* and Cousins *I* bands and in multiple measurements in the Cousins *R* band. An additional *R*-band observation on UT 1998 May 22 did not detect the afterglow, placing an upper limit of $R > 24.0$ on its magnitude. Table 1 gives the details of these observations, and Figure 1 displays the USNO *R*-band detection of the afterglow. Based on these CCD frames and the

[3] A similar analysis for GRB 980519 is presented by Halpern et al. (1999) and was published during the refereeing process of this paper.

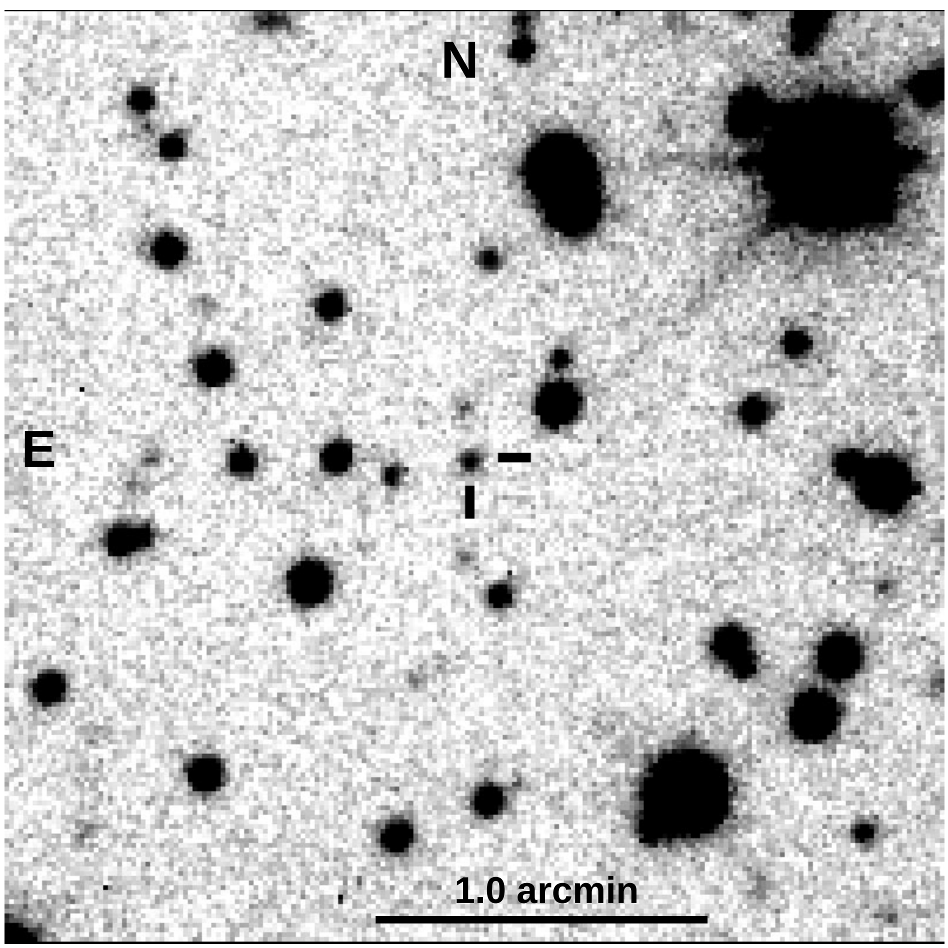

FIG. 1.—*R*-band image of the GRB 980519 field taken with the USNO, Flagstaff Station, 1 m telescope UT 1998 May 20. The image consists of co-added 10 minute exposures beginning at UT 0335 and totaling 120 minutes of integration time. North is at the top, east is to the left, and a scale bar is shown. The optical afterglow is marked.

TABLE 2

SUMMARY OF GRB 980519 OPTICAL OBSERVATIONS

Filter (1)	Date (UT 1998 May) (2)	Mag ± σ(Mag) Observed (3)	Corrected (4)	References (5)
B	20.023	20.95 ± 0.25	20.95 ± 0.25	1
	20.4485	22.53 ± 0.14	22.61 ± 0.17	2
	21.448	> 22.9	> 23.0	2
V	20.2572	21.29 ± 0.20	21.29 ± 0.20	3
	20.466	21.74 ± 0.16	21.95 ± 0.17	2
	21.476	> 22.0	> 22.2	2
R	20.1625	20.28 ± 0.10	20.28 ± 0.10	3
	20.2289	20.68 ± 0.14	20.68 ± 0.14	3
	20.2872	20.79 ± 0.14	20.79 ± 0.14	3
	20.31	20.9 ± 0.2	20.8 ± 0.2	4
	20.4	21.07 ± 0.25	21.04 ± 0.25	5
	20.44	21.20 ± 0.03	21.18 ± 0.03	6
	20.4451	21.09 ± 0.13	21.09 ± 0.13	3
	20.48	21.57 ± 0.09	21.48 ± 0.09	7
	21.469	23.48 ± 0.2	23.39 ± 0.2	8
	21.6	23.10 ± 0.13	23.01 ± 0.13	8
	22.2433	> 24.0	> 24.0	3
	79.516	26.1 ± 0.30	26.0 ± 0.30	7
	85.41	26.05 ± 0.22	26.05 ± 0.22	10
I	19.88	18.48 ± 0.1	18.56 ± 0.1	11
	20.00	19.05 ± 0.03	19.13 ± 0.04	11
	20.1899	20.39 ± 0.15	20.39 ± 0.15	3
	20.31	20.1 ± 0.3	20.2 ± 0.3	4
	20.43	20.86 ± 0.11	20.79 ± 0.12	7
	20.436	21.46 ± 0.1	20.46 ± 0.2	12
	20.98	21.64 ± 0.2	21.72 ± 0.2	11
	21.17	21.64 ± 0.1	21.72 ± 0.1	11
	21.35	21.9 ± ??	21.8 ± ??	13
	21.43	> 21.6	> 21.5	8
	22.332	> 21.0	> 20.9	13
	90.396	> 24.5[a]	> 24.4	9

[a] Gunn-I filter observation.

REFERENCES.—(1) Leibowitz & Ibbetson 1998; (2) Gal et al. 1998a; (3) This paper; (4) Kemp & Halpern 1998; (5) Diercks & Morgan 1998; (6) Deutsch 1998; (7) Bloom et al. 1998a; (8) Gal et al. 1998b; (9) Bloom et al. 1998b; (10) Sokolov et al. 1998; (11) Hjorth et al. 1998; (12) Djorgovski et al. 1998; (13) Castander et al. 1998.

USNO-A v2.0 Catalog of Astrometric Standards (Monet et al. 1998), we calculate the position of the afterglow to be $\alpha(\mathrm{J2000}) = 23^{\mathrm{h}}22^{\mathrm{m}}21\overset{\mathrm{s}}{.}55 \pm 0\overset{\mathrm{s}}{.}03$, $\delta(\mathrm{J2000}) = 77°15'43'' \pm 0\overset{''}{.}1$.

Preliminary reductions of the UT 1998 May 20 R-band observations have previously been reported in Vrba et al. (1998). Our photometry has subsequently been improved by using the secondary standards given by Henden et al. (1998). The complete set of our final photometry and that previously reported in the literature is given in Table 2. For each of the photometry sets from the literature there was enough information given regarding observed values of "local standard" stars such that an offset to the system of Henden et al. (1998) could be made. The corrected values of all the observations are given in column (4). The given errors include the uncertainties of the offsets. The final column provides the references for all of the photometry. We use the corrected values, which are on the Johnson/Cousins systems, throughout the remainder of this paper.

3. ANALYSIS

The combined data of Table 2 are sufficient to produce light curves in the R and I bands and to fit power laws to the data. In order to fit the light curve of the GRB 980519 afterglow itself, we first needed to correct the observed magnitudes, μ, by subtracting, in flux, the brightness of the underlying galaxy, μ_b, producing measures of the afterglow alone, μ'. This is straightforward for the R-band data as photometry was obtained in that band of the galaxy itself, well after the afterglow had faded below the galaxy light level. Sokolov et al. (1998) measured $R = 26.05 \pm 0.22$ from combined photometry obtained on UT 1998 July 23 and 24, while Bloom et al. (1998b) determined $R = 26.0 \pm 0.3$ on UT 1998 July 18; both values have been transformed to the system of Henden et al. (1998). The weighted average of these is $R = 26.03 \pm 0.18$, where the error reflects the minimum error based on the individual errors.

For the I-band data, no separate measurements of the galaxy were obtained after the afterglow had faded, nor are there any estimates of the galaxy morphological type due to its faintness. The $R-I$ color range of normal galaxies is $R-I \approx 0.7 \pm 0.2$, based on the work of Frei & Gunn (1994) and recent results from the Sloan Digital Sky Survey (J. R. Pier 1998, private communication). Combining this color range with the above R-band magnitude gives $I = 25.33 \pm 0.27$ as a probable I-band magnitude for the galaxy. There is some evidence that the underlying/host galaxies of other GRBs may be bluer than normal galaxies. In this case we will have overestimated the contribution of the galaxy in the I band and slightly steepened the resulting afterglow light curve. We also note that Bloom et al. (1998b) report an upper limit of $I_{\mathrm{Gunn}} > 24.5$ on UT 1998 July 29, which at least rules out galaxies redder than about $R-I = 1.5$.

The resulting afterglow magnitudes, μ', were then fitted using weighted least squares with a power law of the form

$$\mu' = -2.5(-\alpha)\log_{10} T + \mu_0 , \tag{2}$$

where α is the power-law index, T is the time of observation after some fiducial time t_0, μ_0 is the fiducial brightness, and

$$\mu' = -2.5 \log_{10}(10^{-\mu/2.5} - 10^{-\mu_b/2.5}) . \tag{3}$$

It is normally assumed that $t_0 = t_{\mathrm{GRB}}$, thus $T = t_{\mathrm{obs}} - t_{\mathrm{GRB}}$. In this case (BATSE Trigger 6764), t_{GRB} is 468.34 hours past UT 1998 May 0, corresponding to UT 1998 May 19.51403. Upper limit observations were excluded from the fit.

The R- and I-band light curves are displayed in the upper panels of Figures 2 and 3, respectively. In these figures the observed magnitudes, μ, are plotted against log T. The triangles represent USNO data, circles represent data from the literature, and open symbols represent upper limit observations. The best-fit power laws are also shown, where we have added the flux from the galaxy back into the fits so that the lines representing the power laws are consistent with the observed data. The bottom panels of these figures show the residuals from the best-fit power laws. The best-fit power-law slopes are $\alpha_R = 2.30 \pm 0.12$ and $\alpha_I = 2.05 \pm 0.07$. No obvious systematic deviations from the power-law fits are seen. However, statistical tests for second-order terms in the light curve are problematic with so few data points.

A short word of caution should be added regarding the common assumption that $t_0 = t_{\mathrm{GRB}}$. While this appears to be a natural assumption, and when consistently applied, allows direct comparison of afterglow slopes, there is no astrophysically compelling reason why the asymptote of the afterglow light curve should be at the moment of the

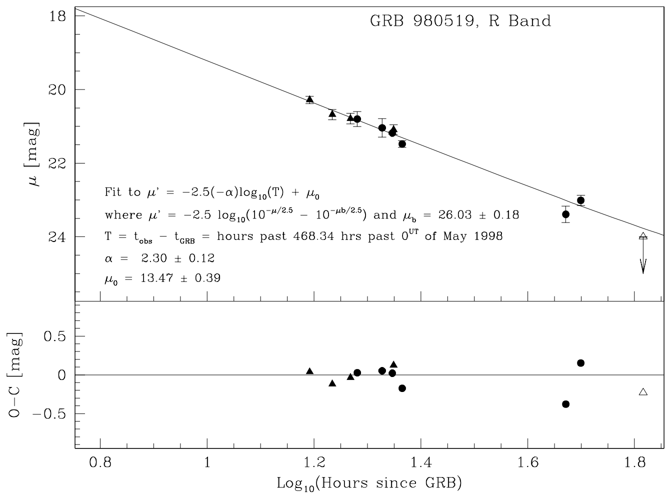

FIG. 2.—Upper panel shows the R-band afterglow light curve of GRB 980519. The triangular data points are from USNO, while the circular data points are taken from the literature cited in Table 2. The open data points are upper limits. 1 σ error bars are shown in all cases. Also shown is the best-fit power law of slope $\alpha_R = 2.30$, assuming $t_0 = t_{\rm GRB}$. The underlying galaxy flux has been returned to the fit so that the fit agrees with the observed data points which are also plotted. The bottom panel shows the residuals of the data points from the best-fit power law.

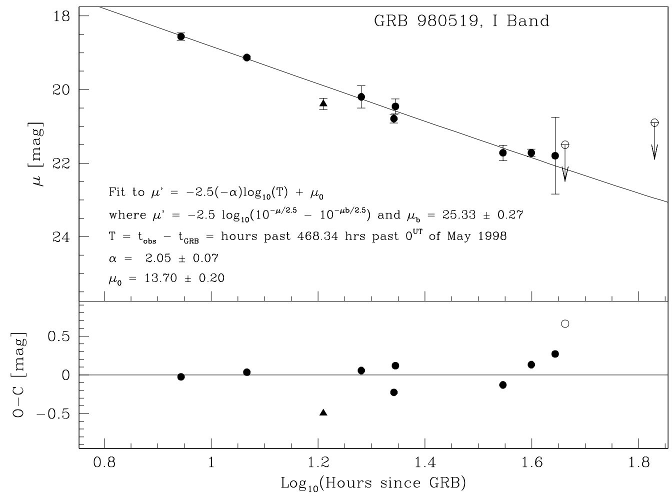

FIG. 3.—Same as Fig. 2, except for I-band data and best-fit power law of slope $\alpha_I = 2.05$.

gamma-ray trigger, especially since the light curves are not yet well understood soon after the GRB (see § 1). Furthermore, the best-fit value of α is relatively sensitive to the choice of t_0. As an example, we allowed both α and t_0 as free parameters and refit the data of this paper with results for the I band: $\alpha = 2.25 \pm 0.46$, $t_0 = 468.90 \pm 5.21$ hours past UT 1998 May 0; and for the R band: $\alpha = 1.72 \pm 0.22$, $t_0 = 471.20 \pm 1.75$ hours past UT 1998 May 0. This demonstrates that α may not be as well constrained as formal fitting errors indicate when t_0 is fixed and that, in some cases, α can be a fairly strong function of the choice of t_0.

4. DISCUSSION

As opposed to prompt radiation, afterglows do not provide direct information regarding the actual cause of the GRBs. Afterglow observations do provide direct information about how the GRB energy is dissipated as it interacts with the circumburst medium. As mentioned in § 1, several similar discussions have been published that describe the temporal and spectral behavior of afterglows caused by synchrotron emission due to the deceleration of relativistic electrons. In the following discussion, we use the models of Sari et al. (1998) but the nomenclature of Groot et al. (1998). Depending on the time and energy regimes during which observations are made, different temporal power-law slopes (α) and spectral slopes (β) will be observed (Sari et al. 1998) in the relation

$$F(t, \nu) = F_0 t^{-\alpha} \nu^{-\beta} . \qquad (4)$$

In these models α and β are both unique functions of the power-law exponent of the electron Lorentz factor distribution. In the case where no breaks are observed in the light curve, such as for GRB 980519, α should simply predict β and thus provide a direct test of these models. We will consider the same cases as did Groot et al. (1998) in order to compare our results with those of GRB 980326, which is the only other afterglow with α as steep as that of GRB 980519.

The peak frequency (ν_m) and cooling frequency (ν_c) are both defined in Sari et al. (1998). In the case where, at the time of observation, $\nu_m < \nu_{\rm obs}$ and $\nu_c < \nu_{\rm obs}$, $\beta = (2\alpha + 1)/3$. From the R- and I-band observations, the predictions from α for GRB 980519 are $\beta_R = 1.87 \pm 0.08$ and $\beta_I = 1.70 \pm 0.05$. In the case where, at the time of observation, $\nu_m < \nu_{\rm obs}$ but $\nu_c > \nu_{\rm obs}$, $\beta = 2\alpha/3$. From the R- and I-band observations, this predicts $\beta_R = 1.53 \pm 0.08$ and $\beta_I = 1.37 \pm 0.05$.

In the case of GRB 980519, we have enough quality optical data between the B and I bands to provide some meaningful constraints on a direct determination of β, despite the small baseline in observed $\nu_{\rm obs}$. Figure 4 provides a summary of the observed values of β. The solid line represents the calculated values of β based on the best-fit power-law slopes in the R and I bands. The dashed lines represent the 1 σ limits to this determination. The $B-R$ and $B-I$ points are based on the two B-band detections and the R and I magnitudes predicted by the best-fit R- and I-band power laws at the times of the B-band observations. The $V-R$ and $V-I$ points are determined in a similar way. The single $B-V$ point is based on the nearly simultaneous B- and V-band observations obtained near UT 1998 May 20.45. We note that since $\alpha_R \neq \alpha_I$, our calculations of β based on the R- and I-band power laws will perforce predict temporal evolution of β. However, as the 1 σ error lines of this calculation in Figure 4 and the error bars of the individual data points indicate, there is no statistically significant indication of time evolution of β in any of the data, which is consistent with the simple blast-wave models.

The individual β determinations are consistent with each other and give a formal weighted mean value of $\beta = 1.9 \pm 0.3$. We used the Hakkila et al. (1997) extinction model ($A_V = 0.481$ at $l = 117^\circ.9632$, $b = 15^\circ.2578$) and a standard extinction curve [$R = 3.05$ implies $E(B-V) = 0.158$] to deredden the observations and recalculate β, with the result $\beta = 1.4 \pm 0.3$. This result is in good agreement with the blast-wave models, especially for the case where $\nu_m < \nu_{\rm obs}$, $\nu_c > \nu_{\rm obs}$. However, the corrected values of β are extremely sensitive to the assumed extinction; for these values a change in $E(B-V)$ of only 0.05 will change the corrected β-value by 0.2. GRB 980519 occurred at an intermediate Galactic latitude where Galactic extinction can change significantly over small angular distances

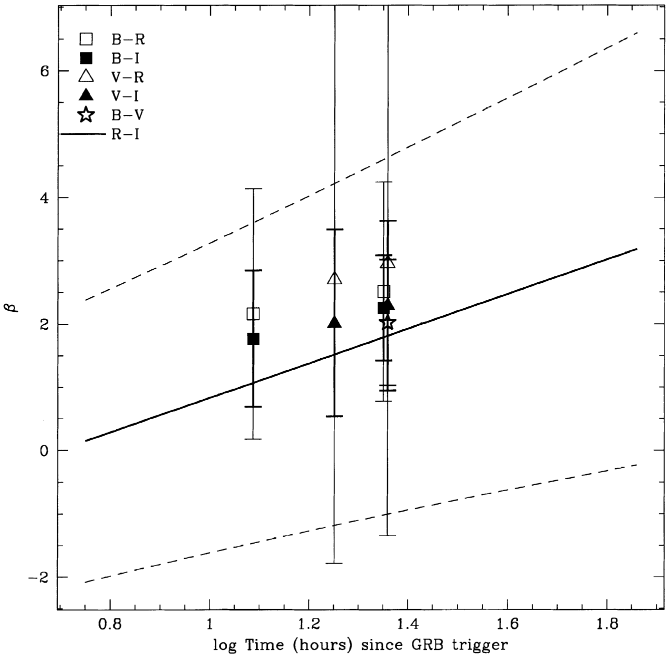

FIG. 4.—Summary of the observed values of the spectral power-law index β. The solid line represents the calculated values of β based on the best-fit temporal power-law slopes, α, in the *R* and *I* bands. The dashed lines represent the 1 σ limits to this determination. The $B-R$ and $B-I$ points are based on the two *B*-band detections and the *R* and *I* magnitudes predicted by the best-fit *R* and *I* power laws at the times of the *B*-band observations. The $V-R$ and $V-I$ points are determined in a similar way. The single $B-V$ point is based on the nearly simultaneous *B*- and *V*-band observations obtained near UT 1998 May 20.45.

and the use of large-scale extinction studies can be risky. The Schlegel, Finkbeiner, & Davis (1998) extinction maps, for instance, predict $E(B-V) = 0.267$ at the same Galactic coordinates, with a resulting corrected β-value of 1.0 ± 0.3. The most that can be stated is that the observed values of β for GRB 980519 are not inconsistent with those predicted by the Sari et al. (1998) models for these regimes.

Table 3 compares the *R*-band slope for GRB 980519 with eight other well-determined *R*-band power-law slopes. Most of the afterglows faded more slowly than $\alpha \approx 1.4$. Only GRB 980326 had a rate of decline comparable to GRB 980519, at $\alpha = 2.10 \pm 0.13$ (Groot et al. 1998), for which the above models predict β-values between 1.40 and 1.03. The Groot et al. (1998) observationally determined value of $\beta = 0.66 \pm 0.70$ is consistent with the model values, albeit with large uncertainty. Thus, the two GRB afterglows with extreme values of α, 980519 and 980326, both appear to be consistent with a simple blast-wave model within the limits that relatively sparse data can provide.

There appears to be little resemblance between the intrinsic GRB properties of 980519 and 980326 that might link their similarly steep afterglow declines. GRB 980519 had a duration of approximately 60 s, a fluence of 2.5×10^{-5} ergs cm^{-2}, and a peak flux placing it among the brightest 12% of GRBs observed by BATSE (Connaughton 1998), whereas GRB 980326 had a duration of only about 5 s and a fluence of only 1×10^{-6} ergs cm^{-2}(Briggs et al. 1998). Groot et al. (1998) have pointed out that the peak of the νF_ν spectrum (E_p) for GRB 980326 was only 47 ± 5 keV, placing it in the bottom 4% of the distribution of GRB E_p-values tabulated by Mallozzi et al. (1998). By contrast, GRB 980519 had an E_p-value of 284 ± 50 keV (R. M. Kippen & R. D. Preece 1999, private communication), which is near the peak of the distribution of E_p-values (Mallozzi et al. 1998).

These dissimilarities are not unexpected as afterglows are thought to be a product of the GRBs and their interaction with the circumburst medium. Chevalier & Li (1999) compute afterglow light curves for constant density circumburst media (appropriate for mergers of compact objects where the surrounding medium is not disturbed before the GRB) and for media where density $\propto r^{-2}$ (appropriate for supernova models where the medium is affected by a strong Wolf-Rayet stellar wind prior to the supernova/GRB). These models predict that the r^{-2} distributions produce steeper light curves. Chevalier & Li (1999) present arguments that both GRB 980326 and GRB 980519 could have been associated with supernovae.

TABLE 3

COMPARISON OF *R*-BAND POWER-LAW SLOPES

GRB	α	$\sigma(\alpha)$	References
980519......	2.30	0.12	1
980326......	2.10	0.13	2
980703......	1.39	0.3	3
980613......	1.3	...	4
980329......	1.28	0.19	5
971214......	1.22	0.2	6
970228......	1.17	0.04	7
970508......	1.141	0.014	8
990123......	1.12	0.03	9

REFERENCES.—(1) This paper; (2) Groot et al. 1998; (3) Castro-Tirado et al. 1999; (4) Halpern & Fesen 1998; (5) Reichart et al. 1999; (6) Kulkarni et al. 1998; (7) Pian et al. 1998; (8) Galama et al. 1998b; (9) Galama et al. 1999.

5. CONCLUSIONS

The nine well-observed GRB afterglows (Table 3) show strong support for simple blast-wave models wherein the afterglows are produced as a relativistic shock wave decelerates as it encounters the interstellar medium. The rate of decline of seven of the afterglows falls in a narrow range of power-law exponent α between 1.1 and 1.4. Two are much steeper, with α between 2.1 and 2.3, yet without any distinguishing GRB characteristics. It is clear just from these few examples that many dozens or hundreds of afterglow observations will be needed to characterize afterglow properties. Planned space missions offer prospects of fast and accurate localizations of hundreds of GRBs in the near future.

REFERENCES

Akerlof, C. W. & McKay, T. A. 1999, GCN Circ. 205 (http://gcn.gsfc.nasa.gov/gcn/gcn3/205.gcn3)
Bloom, J. S., Djorgovski, S. J., Gal, R. R., Kulkarni, S. R., & Kelly, A. 1998a, GCN Circ. 87 (http://gcn.gsfc.nasa.gov/gcn/gcn3/087.gcn3)
Bloom, J. S., Kulkarni, S. R., Djorgovski, S. G., Gal, R. R., Eichelberger, A., & Frail, D. A. 1998b, GCN Circ. 149 (http://gcn.gsfc.nasa.gov/gcn/gcn3/149.gcn3)
Boella, G., Butler, R. C., Perola, G. C., Piro, L., Scarsi, L., & Bleeker, J. A. M. 1997, A&AS, 122, 299
Briggs, M. S., Richardson, G., Kippen, M., & Woods, P. M. 1998, IAU Circ. 6856, 1
Castander, F. J., Evans, R., Reichart, D. E., Lamb, D. Q., & Wild, W. 1998, GCN Circ. 90 (http://gcn.gsfc.nasa.gov/gcn/gcn3/090.gcn3)
Castro-Tirado, A. J., et al. 1999, ApJ, 511, L85

Chevalier, R. A., & Li, Z.-Y. 1999, ApJ, 520, L29
Connaughton, V. 1998, GCN Circ. 86 (http://gcn.gsfc.nasa.gov/gcn/gcn3/086.gcn3)
Deutsch, E. 1998, GCN Circ. 82 (http://gcn.gsfc.nasa.gov/gcn/gcn3/082.gcn3)
Diercks, A., & Morgan, J. 1998, GCN Circ. 91 (http://gcn.gsfc.nasa.gov/gcn/gcn3/091.gcn3)
Djorgovski, S. G., Gal, R. R., Kulkarni, S. R., Bloom, J. S., & Kelly, A. 1998, GCN Circ. 79 (http://gcn.gsfc.nasa.gov/gcn/gcn3/079.gcn3)
Frei, Z., & Gunn, J. E. 1994, AJ, 108, 1476
Gal, R. R., Bloom, J. S., Djorgovski, S. G., & Kulkarni, S. R. 1998a, GCN Circ. 92 (http://gcn.gsfc.nasa.gov/gcn/gcn3/092.gcn3)
Gal, R. R., Bloom, J. S., Steidel, C., Adelberger, K. L., Djorgovski, S. G., & Kulkarni, S. R. 1998b, GCN Circ. 88 (http://gcn.gsfc.nasa.gov/gcn/gcn3/088.gcn3)
Galama, T. J. 1999, Nature, 398, 394
Galama, T. J., et al. 1998a, Nature, 395, 670
———. 1998b, ApJ, 497, L13
Groot, P. J., et al. 1998, ApJ, 502, L123
Hakkila, J. H., Myers, J. M., Stidham, B. J., & Hartmann, D. H. 1997, AJ, 114, 2043
Halpern, J. P., & Fesen, R. 1998, GCN Circ. 134 (http://gcn.gsfc.nasa.gov/gcn/gcn3/134.gcn3)
Halpern, J. P., Kemp, J., Piran, T., & Bershady, M. A. 1999, ApJ, 517, L105
Henden, A. A., Vrba, F. J., Luginbuhl, C. B., Canzian, B., Levine, S. E., Guetter, H. H., & Munn, J. A. 1998, GCN Circ. 96 (http://gcn.gsfc.nasa.gov/gcn/gcn3/096.gcn3)
Hjorth, J., Jaunsen, A. O., Kjernsmo, K., & Pedersen, H. 1998, GCN Circ. 84 (http://gcn.gsfc.nasa.gov/gcn/gcn3/084.gcn3)
Jaunsen, A. O., Hjorth, J., Andersen, M. I., Kjernsmo, K., Pedersen, H., & Palazzi, E. 1998, GCN Circ. 78 (http://gcn.gsfc.nasa.gov/gcn/gcn3/078.gcn3)
Kemp, J., & Halpern, J. 1998, GCN Circ. 80 (http://gcn.gsfc.nasa.gov/gcn/gcn3/080.gcn3)
Kulkarni, S. R., et al. 1998, Nature, 393, 35
Leibowitz, E., & Ibbetson, P. 1998, GCN Circ. 124 (http://gcn.gsfc.nasa.gov/gcn/gcn3/124.gcn3)
Lidman, C., et al. 1998, IAU Circ. 6895
Mallozzi, R. S., Pendelton, G. N., Paciesas, W. S., Preece, R. D., & Briggs, M. S. 1998, in AIP Conf. Proc. 428, Fourth Huntsville Symp. on Gamma-Ray Bursts, ed. C. A. Meegan, T. M. Koshut, & R. D. Preece (New York: AIP), 273
Masetti, N., Palazzi, E., Pian, E., Frontera, F., Bartolini, C., Guarnier, A., Piccioni, A., Valentini, G., & Costa, E. 1999 GCN Circ. 233 http://gcn.gsfc.nasa.gov/gcn/gcn3/233.gcn3)
Mészáros, P., & Rees, M. J. 1997, ApJ, 476, 232
Monet, D., et al. 1998, USNO-A v2.0: A Catalog of Astrometric Standards (Flagstaff: USNO)
Paczynski, B. 1991, Acta Astron., 41, 257
———. 1998, ApJ, 494, L45
Pian, E., et al. 1998, ApJ, 492, L103
Piro, L. 1998a, GCN Circ. 74 (http://gcn.gsfc.nasa.gov/gcn/gcn3/074.gcn3)
———. 1998b, GCN Circ. 75 (http://gcn.gsfc.nasa.gov/gcn/gcn3/075.gcn3)
Reichart, D. E., et al. 1999, ApJ, 517, 692
Sari, R., Piran, T., & Narayan, R. 1998, ApJ, 497, L17
Schlegel, D. J., Finkbeiner, D. P., & Davis, M. 1998, ApJ, 500, 525
Sokolov, V., Zharikov, S., Palazzi, E., & Nicastro, L. 1998, GCN Circ. 148 (http://gcn.gsfc.nasa.gov/gcn/gcn3/148.gcn3)
Tinney, C., Stathakis, R., & Cannon, R. 1998, IAU Circ. 6896
Vrba, F. J., Canzian, B., Levine, S. E., Guetter, H. H., Henden, A. A., Luginbuhl, C. B., Munn, J. A., Hartmann, D. H., & Jennings, M. C. 1998, GCN Circ. 83 (http://gcn.gsfc.nasa.gov/gcn/gcn3/083.gcn3)
Wijers, R. A. M. J., Rees, M. J., & Mészáros, P. 1997, MNRAS, 288, L51